

Machine Learning of Potential-Energy Surfaces Within a Bond-Order Sampling Scheme

Daniele Licari, Sergio Rampino(✉), and Vincenzo Barone

Scuola Normale Superiore, Piazza dei Cavalieri 7, 56126 Pisa, Italy
sergio.rampino@sns.it

Abstract. Predicting the values of the potential energy surface (PES) for a given chemical system is essential to running the associated dynamics and modeling its evolution in time. To the purpose of modeling chemical reactions involving few atoms, this task is usually accomplished by fitting or interpolating a set of energies computed at different nuclear geometries through accurate, though computationally demanding, quantum-chemical calculations. Among the several approaches for choosing an appropriate set of geometries and energies, a new scheme has been recently proposed (Rampino S, J Phys Chem A 120:4683–4692, 2016) which is based on a regular sampling in a space-reduced bond-order (SRBO) domain rather than in the more conventional bond-length (BL) domain. In this work we address the performances of four machine-learning (ML) models, as opposed to pure mathematical fitting or interpolation schemes, in predicting the PES of a three-atom system modeling an atom-diatom exchange reaction when coupled to the SRBO sampling scheme. The models (two ensemble-learning, an automated ML, and a deep-learning one), trained on both SRBO and BL datasets, are shown to perform better than popular fitting or interpolation schemes and to give the best results if coupled to SRBO data.

Keywords: Potential energy surface · Space reduced bond order · Atom diatom reactions · Machine learning · Deep learning · Neural networks

1 Introduction

Within the Born-Oppenheimer approximation, the dynamic modeling of a chemical system requires knowledge of the associated potential-energy surface (PES), i.e. the electronic energy (usually the ground-state one) as a function of the

The research leading to these results has received funding from Scuola Normale Superiore through project 'DIVE: Development of Immersive approaches for the analysis of chemical bonding through Virtual-reality Environments' (SNS18_B_RAMPINO) and program 'Finanziamento a supporto della ricerca di base' (SNS_RB_RAMPINO).

© Springer Nature Switzerland AG 2019
S. Misra et al. (Eds.): ICCSA 2019, LNCS 11624, pp. 388–400, 2019.
https://doi.org/10.1007/978-3-030-24311-1_28

nuclear coordinates. For a given a nuclear geometry, this can be accurately computed through high-level *ab initio* methods. However, performing such single-point calculations for all the geometries needed by the dynamics simulation may become computationally demanding and it is often convenient, if not mandatory, to be able to predict the PES on the basis of a limited set of computed energies. For chemical reactions involving three or four atoms, for which exact quantum-dynamics calculations are feasible, a number of methods have been proposed over the past decades based on mathematical fitting or interpolation schemes (see for instance Ref. [1] for a comprehensive review). More recently, the advent of machine learning (ML) has introduced a new class of powerful methods which have been successfully used also for modeling potential-energy surfaces [2–5] and have established as a robust alternative to pure mathematical fitting or interpolation methods.

When using either fitting/interpolation schemes or ML models, a central problem remains that of the choice of a minimal, most informative set of nuclear geometries at which the *ab initio* energies shall be computed. One of the authors recently faced this problem during the assembly of the grid-empowered molecular simulator GEMS [6–10] for the *a priori* modeling of elementary reactive processes [11–14], with a special focus on atom-diatom exchange reactions of the type

$$\mathrm{A} + \mathrm{BC} \rightarrow \mathrm{AB} + \mathrm{C}. \tag{1}$$

GEMS is articulated in a workflow combining electronic-structure, PES-fitting and quantum-dynamics calculations thanks to the definition of a common data format [15,16] for coordinated execution on the distributed platform of the European Grid Infrastructure (EGI) [17]. GEMS has been successfully used to study the dynamics and compute the reactive probabilities/cross sections and rate coefficients of atom-diatom reactions such as Li + FH [14], N + N_2 [18,19], O + O_2 [20,21], and C + CH^+ [22–24]. In this context, one of us has recently proposed an efficient scheme [25] that has built-in a metric based on the chemical concept of bond order and that is based on a regular sampling in a space-reduced bond-order (SRBO) domain rather than in the more conventional bond-length (BL) one. Using both a global fitting and a local interpolation scheme, the SRBO sampling proved to perform much better than the conventional BL one in converging the predicted PES values to the computed *ab initio* ones with increasing number of grid points.

On these grounds, and motivated by the growing success of ML in many branches of science, we decided to evaluate the performances of several ML techniques in predicting the PES for processes of the type of Reaction 1 when coupled to the SRBO sampling scheme. Accordingly, in this work we address the predictive accuracy of four ML models (two ensemble-learning, an automated ML, and a deep learning one) trained on both SRBO and BL datasets and compare it with that of both a global-fitting and a local-interpolation scheme. To this purpose, we choose the PES of a three-hydrogen system modeling the simplest atom-diatom chemical reaction, $H + H_2 \rightarrow H_2 + H$. In Sect. 2, the SRBO

sampling scheme is briefly reviewed. In Sect. 3, the considered ML models are described and their performances are discussed. In Sect. 4, some conclusions are given and future work is outlined.

2 Bond-Order Sampling and Computational Details

A suitable set of internal coordinates for modeling Reaction 1 is made of the bond-length (BL) variables r_1 and r_2 of the reactant (BC) and product (AB) diatomic, respectively, plus the angle ϕ formed by the two bonds. A simple and practiced recipe for building the above-mentioned set of energies, is to perform a regular sampling on a three-dimensional grid in r_1, r_2, and ϕ, once boundaries $r_{\min}$ and $r_{\max}$ have been defined for a given r in order to exclude the strongly repulsive (dynamically inaccessible) and the near-asymptotic regions (we shall refer to this sampling scheme as to the bond-length, BL, one). Based on the concept of 'bond order' introduced by Pauling more than sixty years ago [26] and revived in the context of PES fitting by Laganà and García [27–30], one of us has recently proposed an alternative sampling scheme that better accounts for the nature of the underlying chemical process governed by the PES under study [25]. The approach (so-called space-reduced bond-order, SRBO) is based on a space-reduced formulation of the so-called bond-order variables and shall be briefly reviewed in the following for the reader's convenience.

Bond-order (BO) variables are defined as the exponential of the weighed diatomic displacement

$$n = e^{-\beta(r-r_e)} \tag{2}$$

where β is a constant related to one or more diatomic force constants, r_e is the equilibrium distance and r is the internuclear distance, or BL variable, of the diatom. BO variables have the following appealing properties: (1) the BO space has origin at infinite internuclear distances and a finite limiting value of $e^{\beta r_e}$ corresponding to null internuclear distance (collapsed atoms) (2) the attractive and repulsive regions of the diatom configuration space are confined in the (0, 1) and (1, $e^{\beta r_e}$) range, respectively, with unity in BO space representing the equilibrium point. BO variables have been used in formulating polynomial representations of PESs [27,28] and rotating diatomic-like ones (like the rotating bond-order, ROBO, [29] and the largest-angle generalization of the rotating bond-order, LAGROBO [30]). In addition, BO variables have been used for producing relaxed, process-oriented PES representations [21] and developing the related quantum-reactive-scattering formalism [31,32].

A space-reduced formulation of the BO variables can be obtained by relaxing the condition that β is linked to spectroscopic properties, and allowing it to vary until a desired attractive over repulsive space ratio f is reached [25]:

$$f = \frac{1 - n_{\min}}{n_{\max} - 1} = \frac{1 - e^{-\beta(r_{\max}-r_e)}}{e^{-\beta(r_{\min}-r_e)} - 1} \,. \tag{3}$$

In so doing, once f has been fixed the same space relation between the attractive and repulsive region of configuration space will hold for any diatom, and f can be chosen to best suit the problem at hand. Test calculations reported in Ref. [25] show that an optimal value of f for the sampling of configuration space for a reactive processes is two (attractive region doubly represented with respect to the repulsive one). In Ref. [25], an automated way of setting $r_{\min}$ and $r_{\max}$ based on the energy-derivative at the equilibrium point is also suggested.

The SRBO sampling is obtained by taking regular grids in n_1, n_2, and ϕ rather than, as in the BL sampling, r_1, r_2, and ϕ. As clearly shown in Fig. 1, the advantage of a regular sampling in n (SRBO sampling) over that in r (BL sampling) is that, assuming an equal number of points, the SRBO points will distribute according to a 'force'-based metric thus better recovering the overall shape of the interaction potential.

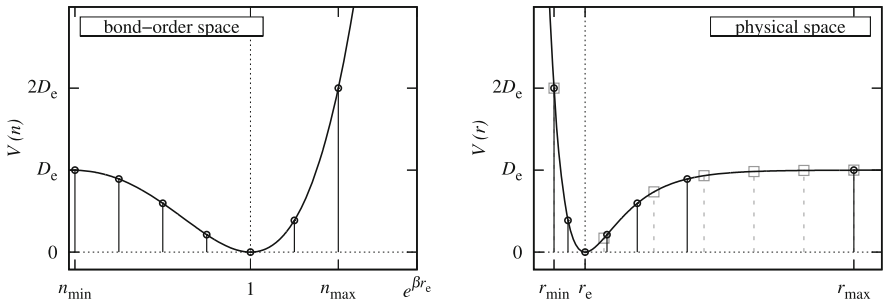

Fig. 1. Energies sampled by a 7-point SRBO ($f = 2$) grid in the bond-order space (left panel) and physical space (right panel). In the right panel, the points of a corresponding 7-point BL grid are also reported as gray squares.

3 Machine Learning of the H_3 Potential-Energy Surface

As already mentioned, we addressed the performances of four ML models in predicting the PES of the H_3 system when coupled to both the SRBO and BL sampling schemes using datasets of incresing size. The energy datasets considered in this work are the same as those of Ref. [25] (to which the reader is referred for a more detailed information), i.e. full configuration interaction (FCI) energies computed with a triple-ζ quality basis set with $r_{\min}$ and $r_{\max}$ set at 0.553 and 8.740 a_0, respectively, and are briefly summarized here. An angular grid of five values ranging from 180° (collinear configuration) to 60° in steps of 30° was set up for the ϕ variable. In the BL sampling, four uniform grids of different size (10, 13, 16, and 19 points) were set for both the r_1 and r_2 BL variables. In the SRBO sampling, analogous 10-, 13-, 16-, and 19-point grids were set in the corresponding n_1 and n_2 defined with $f = 2$. For each of the two sampling schemes (after removing redundant points due to the symmetry of the system

and including the H_3 saddle point) this leads to four datasets of 276, 456, 681, and 951 points ('training sets' hereafter).

The performances of the considered predictive models were evaluated in terms of root-mean-square error (RMSE) of the predicted values with respect to a reference set of energies ('reference set' hereafter) computed on a finer grid of 2951 points obtained with a 25-points BL sampling for both r_1 and r_2 and an angular grid from 180° to 60° in steps of 15° for ϕ.

The four ML models considered herein are described and assessed in the following subsections. In particular, in Subsect. 3.1 we discuss two ensemble-learning models (referenced to as RF and XGB). In Subsect. 3.2 we discuss an automated ML and a deep learning model (referenced to as AS and DL). Our ML algorithms were implemented using the scikit-learn [33] (for RF and XGB), Autosklearn [34] (for AS) and Keras [35] (for DL) software. A complete summary of the results is given in Table 1, which also reports the performances of a global-fitting (Aguado-Paniagua, AP [36,37]) and a local-interpolation (modified Shepard, Sh [38]) scheme evaluated on the same grounds.

Table 1. RMSE with respect to the reference set of the AP, Sh, RF, XGB, AS and DL predictive models using datasets of $N = 276$, 456, 681, and 951 H_3 energies computed through both an SRBO and a BL sampling scheme as detailed in Sect. 2. AP and Sh data taken from Ref. [25].

	RMSE /eV											
	SRBO						BL					
N	AP	Sh	RF	XGB	AS	DL	AP	Sh	RF	XGB	AS	DL
276	0.029	0.123	0.021	0.027	0.019	0.018	1.455	11.636	0.121	0.121	0.088	0.049
456	0.026	0.060	0.010	0.017	0.020	0.011	0.264	3.636	0.029	0.028	0.029	0.036
681	0.027	0.021	0.009	0.016	0.009	0.013	0.144	2.982	0.023	0.024	0.023	0.018
951	0.025	0.016	0.008	0.015	0.008	0.012	0.077	2.407	0.020	0.024	0.015	0.021

3.1 Ensemble-Learning Methods

Ensemble learning methods are based on observation that the aggregate decision made by a group is often better than those of its individual members if specific conditions are satisfied (the wisdom-of-crowds theory [39]). The Random Forest (RF) [40] is an ensemble of decision trees [41] which operate on a random sample of the data outputting mean prediction of the individual trees. This randomness helps to make the model more robust than a single decision tree, and less likely to overfit on the training data. Instead, eXtreme Gradient Boosting (XGB) [42] builds an ensemble of trees by optimizing a differentiable loss function and uses a more regularized model formalization to control over-fitting. Basically, it helps to find a predictor which is a weighed average of all models used. XGB models dominate many data science competitions hosted at Kaggle (https://kaggle.com) as they work very well on conventional, also called tabular or structured, data (as those considered in this article).

Machine-learning models can require several input variables (called hyperparameters) that govern the training process itself. The choice of these parameters highly affects the performance of the models, thus hyperparameter tuning is a crucial task in the definition of a machine-learning model. The traditional way of performing hyperparameter optimization is a grid search which builds a model for each possible combination of all of the hyperparameter values provided and selects the one which produces the best results. This approach requires long execution time because it wastes time evaluating unpromising areas of parameter space. Instead, we used a Bayesian optimization method for hyperparameter tuning of RF and XGB models [43,44] evaluating on training sets.

This automatic approach, based on a probabilistic model for finding optimal hyperparameters, works by building a posterior distribution of functions (Gaussian process) that best describes the function we want to optimize (mean-squared-error, MSE, function). As the number of observations increases, the posterior distribution improves, and the algorithm becomes more confident of which regions of the parameter space are worth exploring and which are not. In our case, the target variable (the energy) to be optimized is measured as the average of MSEs from 5-fold cross-validation (CV) on the training set. A 5-fold CV would re-sample the training and validation sets in a non-overlapping fashion 5 times, such that all of the data is eventually used as training data. The CV error is then estimated by averaging the five resulting MSE estimates (CV is often used to estimate this generalization performance). The optimal hyperparameter values (herein obtained from the hyperparameter configuration space reported in Table 2) are those that have produced the lowest CV error.

As already mentioned, the performances of the RF and XGB models trained on the above defined training sets are reported in Table 1. Both ML models significantly improve the performance of fitting compared to AP and Sh. Predictive error of both methods are remarkably similar, with RF performing somewhat better than XGB. This may be because the RF has fewer parameters to set and therefore it is easier for a Bayesian optimizer to find the best hyperparameters.

Table 2. Configuration spaces of Random Forest and Extreme Gradient Boosting hyperparameters used into Bayesian optimization with 250 iterations.

Model	Hyperparameter name	Values
RF	n_estimators	[10, 2500]
	min_samples_split	[2, 25]
	max_features	[0.1, 0.999]
XGB	n_estimators	[100, 2500]
	learning_rate	[0.05, 0.3]
	max_depth	[3, 10]
	subsample	[2, 25]
	gamma	[0.01, 1.0]

3.2 Automatic Machine Learning and Deep Learning

Finding the best machine-learning algorithm and right data preprocessing steps for a specific dataset is a non-trivial and error-prone task for humans. Many more models are continuously being developed, hyper-parameter tuning is not an easy task, and preprocessing steps (such as data scaling, features selections and missing values) can be necessary to improve the performances. For this reason, automated ML (AutoML) has become a topic of considerable interest in recent years as they can automatically determine a well-performing ML pipeline for a specific dataset.

Existing state-of-the-art AutoML systems include auto-sklearn (AS) [34,45] which wraps 15 regressors/classifiers and 18 preprocessing methods, and exploits recent advances in Bayesian optimization, meta-learning and ensemble construction to search the right learning algorithm and optimize its hyperparameters. Bayesian optimization is used to optimize the hyperparameters of the best pipelines (preprocessing and models) resulting from the meta-learning process. Finally, auto-sklearn builds an ensemble of the 50 best models tested during the global optimization process to improve generalization.

Another ML approach that we tested is based on deep neural networks (NN), also referred to as deep learning (DL), which has raised broad interest due to its strong learning capacity for various problems in many scientific [46,47] and industrial [48] areas. Deep-learning [49] models are composed of multiple processing non-linear modules (called neurons) to lean representation of data with multiple levels of abstraction. Neurons are distributed in multiple layers (hidden layers) and each layer uses the output from the previous layer as input. It learns through an optimizer (e.g. Stochastic Gradient Descent or Adaptive Gradient Methods) which, during the training phase, minimizes an objective function that measures the error (MSE in our case) by computing its gradient vector and modifies the internal adjustable parameters to reduce this error.

Our feed-forward neural network (see a scheme in Fig. 2) takes the three internal coordinates as input, it is composed of 2 hidden layers (each layers contains 20 neurons) and its last node outputs the fitted energy. In general, neurons take several input numbers from the previous layer, apply an activation function to the weighed sum of inputs (weights are the fitting parameters of a NN) and yield the output. In biological processing the signal must exceed a certain threshold to be propagated, in NN this behaviour is simulated by the activation function. The non-linear functions used in our NN include the rectified linear unit (ReLU) $f(z) = \max(0, z)$, commonly used in recent years and Stochastic Gradient Descent as optimizer. Our NN was built with Keras [35] specifying the hyperparameters reported in Table 3 (we use default values for the remaining parameters, for which the reader is referred to the Keras documentation).

Table 3. Hyper-parameters of our neural network.

Name	Values
loss	MSE
optimizer	SGD
epochs	14000
batch_size	50
validation_split	0.2

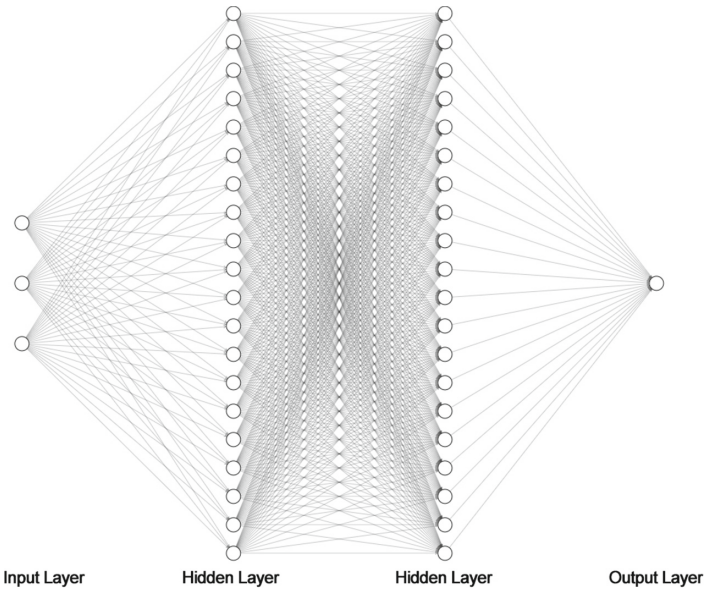

Fig. 2. Our neural-network topology is defined by 3 input nodes (the three internal coordinates), two hidden layers with 20 nodes per layer and one output node (E).

As previously done for the RF and XGB models, the predictive accuracy of the AS and DL models was evaluated in terms of RMSE of the predicted values with respect to the reference set and results are reported in Table 1. The results of these two models are quite similar. DL generalizes better than AS if one uses a training set of 256 points, on the contrary AS has better performances with training data of increasing size. Figure 3 and 4 show the overall performances of all the considered ML models trained with both SRBO (Fig. 3) and BL (Fig. 4) datasets, as compared to the performances of the AP fitting scheme. The SRBO sampling scheme provides great benefit on machine-learning algorithms considerably reducing the RMSE with respect to BL sampling. In addition, the performances of the ML models are considerably better than those of the AP fitting. Considering the performances, the simplicity of setting and the ease of parallelization, the RF on SRBO is the best algorithm for our case study.

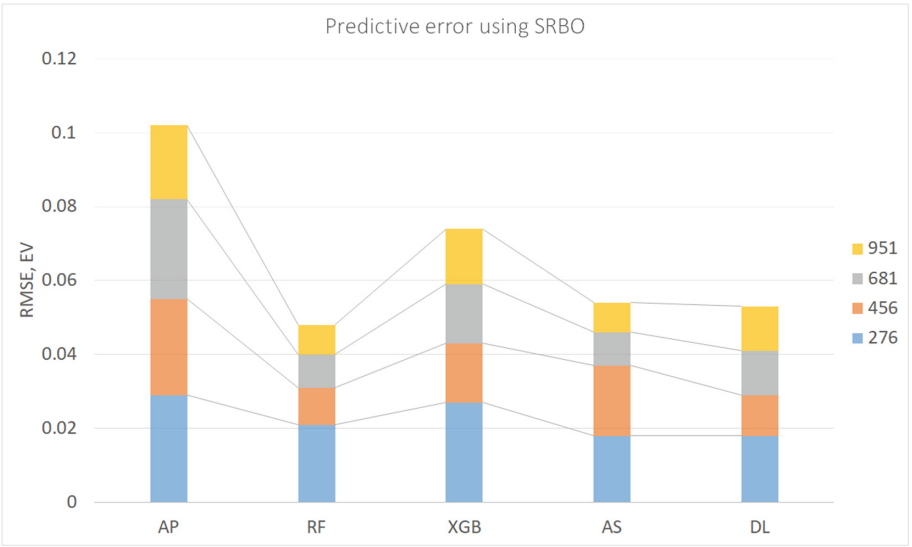

Fig. 3. Overall performances of the considered ML models coupled to the SRBO sampling scheme as compared to those of the AP fitting.

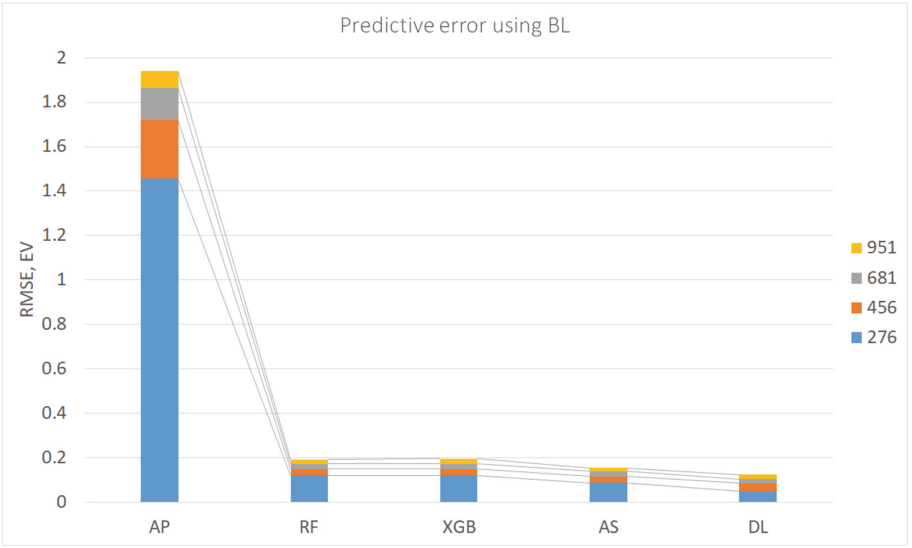

Fig. 4. Overall performances of the considered ML models coupled to the BL sampling scheme as compared to those of the AP fitting.

These results indicate that a combination of an SRBO sampling scheme with state-of-the-art ML methods offers the cheapest and most effective approach to PES fitting for the three-atom reactive systems herein considered.

4 Conclusions

In this paper we assess the performances of four machine-learning (ML) models in predicting the potential-energy surface (PES) of a three-atom chemical reactive process when coupled to the recently proposed space-reduced bond-order (SRBO) configuration sampling scheme, as opposed to the more conventional bond-length (BL) one. After training the ML models (two ensemble-learning, an automated ML, and a deep learning one) with SRBO and BL datasets of increasing size, their performances were evaluated by computing the root-mean-square error (RMSE) of the predicted energy with respect to a larger set of energies, and compared to those of established fitting/interpolation schemes.

Results indicate that for a training set of a given size ML techniques perform better than the considered global-fitting and local-interpolation schemes, and that better results are achieved if an SRBO sampling is adopted rather than a BL one. On the one hand, this confirms the SRBO sampling scheme as a reliable and efficient tool in PES-fitting problems of few-atom reactive systems. On the other hand, these results suggest that one-dimensional SRBO grids can be used as optimal building blocks for multi-dimensional grids in higher-dimensionality problems. Work is in progress in our laboratory to extend these computational approaches to larger systems and to exploit them for an efficient 3D-rendering for visualization purposes and immersive exploration of the PES through state-of-the-art virtual-reality technologies [50,51].

References

1. Jaquet, R.: Interpolation and fitting of potential energy surfaces: concepts, recipes and applications. In: Sax, A.F. (ed.) Potential Energy Surfaces. Lecture Notes in Chemistry, vol. 71, pp. 97–175. Springer, Berlin (1999). https://doi.org/10.1007/978-3-642-46879-7_3
2. Behler, J.: Neural network potential-energy surfaces for atomistic simulations. In: Chemical Modelling: Applications and Theory, vol. 7, pp. 1–41. The Royal Society of Chemistry, Cambridge (2010)
3. Handley, C.M., Popelier, P.L.A.: Potential energy surfaces fitted by artificial neural networks. The J. Phys. Chem. A **114**(10), 3371–3383 (2010)
4. Hughes, Z.E., Thacker, J.C.R., Wilson, A.L., Popelier, P.L.A.: Description of potential energy surfaces of molecules using FFLUX machine learning models. J. Chem. Theor. Comput. **15**(1), 116–126 (2019)
5. Raff, L., Komanduri, R., Hagan, M., Bukkapatnam, S.: Neural Networks in Chemical Reaction Dynamics. Oxford University Press, New York (2012)
6. Laganà, A., Costantini, A., Gervasi, O., Faginas Lago, N., Manuali, C., Rampino, S.: COMPCHEM: progress towards GEMS a grid empowered molecular simulator and beyond. J. Grid Comput. **8**(4), 571–586 (2010)
7. Rampino, S.: Workflows and data models for atom diatom quantum reactive scattering calculations on the Grid. Ph.D. thesis, Università degli Studi di Perugia (2011)
8. Manuali, C., Laganà, A., Rampino, S.: GriF: a grid framework for a web service approach to reactive scattering. Comput. Phys. Commun. **181**(7), 1179–1185 (2010)

9. Rampino, S., Faginas Lago, N., Laganà, A., Huarte-Larrañaga, F.: An extension of the grid empowered molecular simulator to quantum reactive scattering. J. Comput. Chem. **33**(6), 708–714 (2012)
10. Rampino, S., Storchi, L., Laganà, A.: Automated simulation of gas-phase reactions on distributed and cloud computing infrastructures. In: Gervasi, O., et al. (eds.) ICCSA 2017. LNCS, vol. 10406, pp. 60–73. Springer, Cham (2017). https://doi.org/10.1007/978-3-319-62398-6_5
11. Rampino, S., Skouteris, D., Laganà, A., Garcia, E.: A comparison of the isotope effect for the N + N_2 reaction calculated on two potential energy surfaces. In: Gervasi, O., Murgante, B., Laganà, A., Taniar, D., Mun, Y., Gavrilova, M.L. (eds.) Computational Science and Its Applications - ICCSA 2008. Lecture Notes in Computer Science, vol. 5072, pp. 1081–1093. Springer, Berlin Heidelberg (2008)
12. Laganà, A., Faginas Lago, N., Rampino, S., Huarte Larrañaga, F., García, E.: Thermal rate coefficients in collinear versus bent transition state reactions: the N+N_2 case study. Physica Scripta **78**(5), 058116 (2008)
13. Rampino, S., Pirani, F., Garcia, E., Laganà, A.: A study of the impact of long range interactions on the reactivity of N + N_2 using the Grid Empowered Molecular Simulator GEMS. Int. J. Web Grid Serv. **6**(2), 196–212 (2010)
14. Laganà, A., Rampino, S.: A grid empowered virtual versus real experiment for the barrierless Li + FH → LiF + H reaction. In: Murgante, B., et al. (eds.) ICCSA 2014. LNCS, vol. 8579, pp. 571–584. Springer, Cham (2014). https://doi.org/10.1007/978-3-319-09144-0_39
15. Rossi, E., et al.: Code interoperability and standard data formats in quantum chemistry and quantum dynamics: the Q5/D5Cost data model. J. Comput. Chem. **35**(8), 611–621 (2014)
16. Rampino, S., Monari, A., Rossi, E., Evangelisti, S., Laganà, A.: A priori modeling of chemical reactions on computational grid platforms: workflows and data models. Chem. Phys. **398**, 192–198 (2012)
17. EGI: The European grid infrastructure. http://www.egi.eu/. Accessed 27 Feb 2019
18. Rampino, S., Skouteris, D., Laganà, A., García, E., Saracibar, A.: A comparison of the quantum state-specific efficiency of N + N_2 reaction computed on different potential energy surfaces. Phys. Chem. Chem. Phys. **11**, 1752–1757 (2009)
19. Rampino, S., Garcia, E., Pirani, F., Laganà, A.: Accurate quantum dynamics on grid platforms: some effects of long range interactions on the reactivity of N + N_2. In: Taniar, D., Gervasi, O., Murgante, B., Pardede, E., Apduhan, B.O. (eds.) Computational Science and Its Applications - ICCSA 2010. Lecture Notes in Computer Science, vol. 6019, pp. 1–12. Springer, Berlin Heidelberg (2010). https://doi.org/10.1007/978-3-642-12189-0_1
20. Rampino, S., Skouteris, D., Laganà, A.: The O + O_2 reaction: quantum detailed probabilities and thermal rate coefficients. Theor. Chem. Acc.: Theor. Comput. Model. **123**(3/4), 249–256 (2009)
21. Rampino, S., Skouteris, D., Laganà, A.: Microscopic branching processes: the O + O_2 reaction and its relaxed potential representations. Int. J. Quantum Chem. **110**(2), 358–367 (2010)
22. Rampino, S., Pastore, M., Garcia, E., Pacifici, L., Laganà, A.: On the temperature dependence of the rate coefficient of formation of C_2^+ from C + CH^+. Monthly Not. Roy. Astron. Soc. **460**(3), 2368–2375 (2016)
23. Pacifici, L., Pastore, M., Garcia, E., Laganà, A., Rampino, S.: A dynamics investigation of the C + CH^+ → C_2^+ + H reaction on an *ab initio* bond-order like potential. J. Phys. Chem. A **120**(27), 5125–5135 (2016)

24. Rampino, S., Suleimanov, Y.V.: Thermal rate coefficients for the astrochemical process C + CH^+ → C_2^+ + H by ring polymer molecular dynamics. J. Phys. Chem. A **120**(50), 9887–9893 (2016)
25. Rampino, S.: Configuration-space sampling in potential energy surface fitting: a space-reduced bond-order grid approach. J. Phys. Chem. A **120**(27), 4683–4692 (2016)
26. Pauling, L.: Atomic radii and interatomic distances in metals. J. Am. Chem. Soc. **69**(3), 542–553 (1947)
27. Garcia, E., Laganà, A.: Diatomic potential functions for triatomic scattering. Mol. Phys. **56**(3), 621–627 (1985)
28. Garcia, E., Laganà, A.: A new bond-order functional form for triatomic molecules. Mol. Phys. **56**(3), 629–639 (1985)
29. Laganà, A.: A rotating bond order formulation of the atom diatom potential energy surface. J. Chem. Phys. **95**(3), 2216–2217 (1991)
30. Laganà, A., Ochoa de Aspuru, G., Garcia, E.: The largest angle generalization of the rotating bond order potential: three different atom reactions. J. Chem. Phys. **108**(10), 3886–3896 (1998)
31. Laganà, A., Crocchianti, S., Faginas Lago, N., Pacifici, L., Ferraro, G.: A nonorthogonal coordinate approach to atom-diatom parallel reactive scattering calculations. Collect. Czechoslovak Chem. Commun. **68**(2), 307–330 (2003)
32. Rampino, S., Laganà, A.: Bond order uniform grids for quantum reactive scattering. Int. J. Quantum Chem. **112**(7), 1818–1828 (2012)
33. Pedregosa, F., et al.: Scikit-learn: machine learning in Python. J. Mach. Learn. Res. **12**, 2825–2830 (2011)
34. Feurer, M., Klein, A., Eggensperger, K., Springenberg, J., Blum, M., Hutter, F.: Efficient and robust automated machine learning. In: Cortes, C., Lawrence, N.D., Lee, D.D., Sugiyama, M., Garnett, R. (eds.) Advances in Neural Information Processing Systems, vol. 28, pp. 2962–2970. Curran Associates, Inc. (2015)
35. Chollet, F.: Keras (2015). https://github.com/fchollet/keras. Accessed 27 Feb 2019
36. Aguado, A., Paniagua, M.: A new functional form to obtain analytical potentials of triatomic molecules. J. Chem. Phys. **96**(2), 1265–1275 (1992)
37. Aguado, A., Tablero, C., Paniagua, M.: Global fit of ab initio potential energy surfaces I. Triatomic systems. Comput. Phys. Commun. **108**(2–3), 259–266 (1998)
38. Shepard, D.: A two-dimensional interpolation function for irregularly-spaced data. In: Proceedings of the 1968 23rd ACM National Conference, ACM 1968, pp. 517–524. ACM, New York (1968)
39. Surowiecki, J.: The Wisdom of Crowds: Why the Many Are Smarter Than the Few and How Collective Wisdom Shapes Business, Economies, Societies, and Nations. Doubleday & Co, New York (2004)
40. Breiman, L.: Random forests. Mach. Learn. **45**(1), 5–32 (2001)
41. Quinlan, J.R.: Induction of decision trees. Mach. Learn. **1**(1), 81–106 (1986)
42. Chen, T., Guestrin, C.: XGBoost: a scalable tree boosting system. In: Proceedings of the 22nd ACM SIGKDD International Conference on Knowledge Discovery and Data Mining, KDD 2016, pp. 785–794. ACM, New York (2016)
43. Snoek, J., Larochelle, H., Adams, R.P.: Practical Bayesian optimization of machine learning algorithms. In: Proceedings of the 25th International Conference on Neural Information Processing Systems, NIPS 2012, vol. 2, pp. 2951–2959. Curran Associates Inc., USA (2012)
44. Brochu, E., Cora, V.M., de Freitas, N.: A tutorial on Bayesian optimization of expensive cost functions, with application to active user modeling and hierarchical reinforcement learning. eprint arXiv:1012.2599, arXiv.org, December 2010

45. Feurer, M., Eggensperger, K., Falkner, S., Lindauer, M., Hutter, F.: Practical automated machine learning for the AutoML challenge 2018. In: ICML 2018 AutoML Workshop (2018)
46. Esteva, A., et al.: A guide to deep learning in healthcare. Nat. Med. **25**(1), 24–29 (2019)
47. Zou, J., Huss, M., Abid, A., Mohammadi, P., Torkamani, A., Telenti, A.: A primer on deep learning in genomics. Nat. Genet. **51**(1), 12–18 (2019)
48. Nash, W., Drummond, T., Birbilis, N.: A review of deep learning in the study of materials degradation. npj Mater. Degrad. **2**(1), 37 (2018)
49. LeCun, Y., Bengio, Y., Hinton, G.: Deep learning. Nature **521**(7553), 436–444 (2015)
50. Salvadori, A., Fusè, M., Mancini, G., Rampino, S., Barone, V.: Diving into chemical bonding: an immersive analysis of the electron charge rearrangement through virtual reality. J. Comput. Chem. **39**(31), 2607–2617 (2018)
51. Salvadori, A., et al.: A walk through chemistry: exploring potential-energy surfaces with virtual reality (2019, in preparation)